



Research Article

# NON-LINEAR FINITE ELEMENT ANALYSIS OF TIME-VARYING THICKNESS AND TEMPERATURE DURING THE EXTRUSION BLOW MOLDING PROCESS

S. Thusneyapan\*

R. Rugsaj

Department of Mechanical

Engineering,

Faculty of Engineering,

Kasetsart University,

50 Ngam Wong Wan Road, Lat Yao,

Chatuchak, Bangkok, 10900,

Thailand

## ABSTRACT:

*This paper presented the use of non-linear finite element analysis (FEA) software to simulate the extrusion blow molding process. We used MSC.MARC to evaluate the thickness and temperature variation in time during the process. The investigation was done on an axis-symmetric bottle made from high density polyethylene (HDPE). The mathematical model for HDPE used visco-elastic material. Our simulation combined both the mold closing and pressure blowing processes in one event. The FEA result compared with the measured thickness, from the processed bottles was observed. In the thickness analysis, we defined the thickness ratio (TR) of the parison and bottle; and found that, the TR was uniform for the analysis range of the initial parison thickness between  $2.4 \pm 0.2$  mm. When the change of the parison thickness is frequently requested during the design and manufacturing processes, the constant TR can be applied; hence, reduces the analysis time. When the hardening temperature of HDPE is known, the time variation plots of the temperature and thickness are useful for predicting the process times.*

**Keywords:** Parison thickness, extrusion blow molding, FEA, thickness ratio, visco-elastic, HDPE.

## 1. INTRODUCTION

In the manufacturing of hollow components, mainly for liquid containers, the extrusion blow molding is one of the most preferred processes. The process creates products in form of bottle, for containing liquid such as: juice, milk and medicine [1]. The commonly used polymer for this process is the high density polyethylene (HDPE) [2]. During the process, HDPE is heated inside an extruder. The molten HDPE is extruded through the die, and became a warm and soft continuous tube called “parison”. The parison is blown against the surface of the mold to form the shape of the bottle. When the parison contacts the mold surface, the heat is transferred to the mold and cooled the parison. The computer-aided design (CAD) has been used for developing the products; together with the finite element analysis (FEA) for observing the deformation during the process [3-6]. The FEA and numerical methods were used for simulating stretch blow molding process [7-9]. There are two material models for the HDPE parison thickness simulation: hyper-elastic and visco-elastic [10]. The comparison between the hyper-elastic and visco-elastic, for the FEA simulation of the HDPE parison thickness, was studied by Rugsaj et al. [11]. In their comparison, from an axis-symmetric bottle, the thickness error of the hyper-elastic model was less than that of the visco-elastic model by 4.02%. However, their result indicated that the visco-elastic model was less complicated and better for applying to bottles with axis-symmetric and symmetric geometries. Also, the visco-elastic model gave:

\* Corresponding author: S. Thusneyapan  
E-mail address: fengsjt@ku.ac.th



less possibility of divergence, suitable for non-isothermal simulation and less computing time.

In this paper, we selected the visco-elastic material model and combined the thermal property to simulate the variation of thickness and temperature in time during the blowing process of the HDPE parison. The results from the simulation would provide engineers to predict the bottle wall thickness under any initial parison thickness and processing conditions; along with the time required for the HDPE to be hardened.

## 2. MATHEMATICAL MODEL OF VISCO-ELASTIC MATERIAL

The HDPE is a thermoplastic. It is used in the manufacturing of hollow products via an extrusion blow molding machine. The mathematical model of HDPE parison is required for analyzing the changes of the parison thickness and temperature during the blowing process. A suitable material model for the HDPE parison analysis is the visco-elastic model [11].

When HDPE is below its melting temperature, it is characterized by elastic and viscous properties. This type of material is known as visco-elastic material. The visco-elastic material model consists of two mechanical elements; they are spring and damper [12, 13]. The spring property of an elastic element, in term of the stress ( $\sigma_e$ ) and strain ( $\varepsilon_e$ ) is equated by the Hooke's law as Eq. (1), and its time derivative is Eq. (2).

$$\sigma_e = E\varepsilon_e, \quad (1)$$

$$\dot{\sigma}_e = E\dot{\varepsilon}_e, \quad (2)$$

where, the constant  $E$  is the elastic modulus of material.

The damper is a viscous element, which is represented by:

$$\sigma_v = \eta\dot{\varepsilon}_v, \quad (3)$$

where  $\eta$  is the viscosity, and  $\dot{\varepsilon}_v$  is the strain rate, that is

$$\dot{\varepsilon}_v = \frac{d\varepsilon_v}{dt}. \quad (4)$$

When both elastic and viscous elements are connected in series, it is known as Maxwell material model. Under this configuration, the stress of the elastic element ( $\sigma_e$ ) equals to the stress of the viscous element ( $\sigma_v$ ) or

$$\sigma = \sigma_e = \sigma_v. \quad (5)$$

While the superposition of both elements yields the total strain ( $\varepsilon$ ), that is

$$\varepsilon_e + \varepsilon_v = \varepsilon. \quad (6)$$

Also, the derivative with respect to time of Eq. (6) is

$$\dot{\varepsilon}_e + \dot{\varepsilon}_v = \dot{\varepsilon}. \quad (7)$$

The substitution of  $\dot{\varepsilon}_e$  and  $\dot{\varepsilon}_v$ , from Eqs. (2) and (3) respectively, into Eq. (7) gives a first order differential equation as:

$$\frac{\dot{\sigma}}{E} + \frac{\sigma}{\eta} = \dot{\varepsilon}. \quad (8)$$

For  $\dot{\varepsilon} = 0$ , Eq. (8) becomes

$$\dot{\sigma} + \frac{\sigma}{\tau} = 0, \quad (9)$$

where  $\tau$  is the relaxation time, and it is related by

$$\tau = \frac{\eta}{E}. \quad (10)$$

Under the relaxation test, the material is given an initial stress at time equals to zero, or  $\sigma(0) = \sigma_0$ ; then, the change in the stress as a function of time is

$$\sigma(t) = \sigma_0 e^{-t/\tau}. \quad (11)$$

Divide Eq. (11) through by strain  $\varepsilon$ , yields the stress relaxation modulus function  $E(t)$ .

$$E(t) = E_0 e^{-t/\tau}. \quad (12)$$

The stress relaxation modulus function is the variation of the elastic modulus in time  $t$ , or  $E(t)$ . The constant  $E_0$ , is the initial elastic modulus at time equals to zero,  $E(0) = E_0$ .

Since most materials are the combination of several elastic elements (each with  $E_i$ ) and several viscous elements (each with  $\eta_i$ ), the stress relaxation modulus function becomes

$$E(t) = \sum_{i=1}^n E_i e^{-t/\tau_i}, \quad (13)$$

where

$$\tau_i = \frac{\eta_i}{E_i}. \quad (14)$$

Similarly, the shear relaxation modulus function  $G(t)$  is

$$G(t) = \sum_{i=1}^n G_i e^{-t/\Gamma_i}, \quad (15)$$

where  $\Gamma_i$  is the shear relaxation time.

When the temperature,  $T$  is considered for the analysis, the time-temperature shift function,  $a_t$  or  $a_t(T)$  is need. The most well-know equation for determining the  $a_t$  is Williams-Landel-Ferry (WLF) equation; it is defined as shown in Eq. (16).

$$\log [a_t(T)] = -\frac{C_1(T - T_{ref})}{C_2 + (T - T_{ref})}, \quad (16)$$

where:  $a_t(T)$  is time-temperature shift function,  $a_t$  (dimensionless),

$T$  is the temperature ( $^{\circ}\text{C}$ ),

$C_1$  is a temperature coefficient (dimensionless),

$C_2$  is a temperature constant ( $^{\circ}\text{C}$ ),

$T_{ref}$  is a reference temperature ( $^{\circ}\text{C}$ ).

The stress relaxation modulus function of time and temperature  $E(t, T)$  can be expressed with  $a_t$  as:

$$E(t, T) = \sum_{i=1}^n E_i e^{-t/a_i \tau_i}. \quad (17)$$

Similarly, the shear relaxation modulus function of time and temperature,  $G(t, T)$  is

$$G(t, T) = \sum_{i=1}^n G_i e^{-t/b_i \Gamma_i}, \quad (18)$$

where  $b_t$  or  $b_t(T)$  is the shear time-temperature shift function; it is similar to Eq. (16), that is

$$\log [b_t(T)] = -\frac{C_{S1}(T - T_{ref})}{C_{S2} + (T - T_{ref})}, \quad (19)$$

where:  $C_{S1}$  is a shear temperature coefficient (dimensionless),

$C_{S2}$  is a shear temperature constant ( $^{\circ}\text{C}$ ).

### 3. SIMULATION MODELING AND CONDITIONS

#### 3.1 3-D Modeling and finite element modeling

A commercial HDPE bottle was selected for the analysis. The bottle had a capacity of 900 ml. This bottle was basically a cylindrical shape, and it was an axis-symmetric geometry (Fig. 1). The 3-D model of bottle and parison were created by using computer-aided design (CAD) software, Pro/ENGINEER WILDFIRE V3.0. The surface model of the bottle was used as the reference for creating its mold surface (left view of Fig. 2).

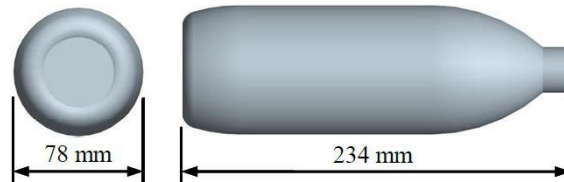


**Fig. 1.** The CAD model of the 900 ml bottle and its primary dimensions.

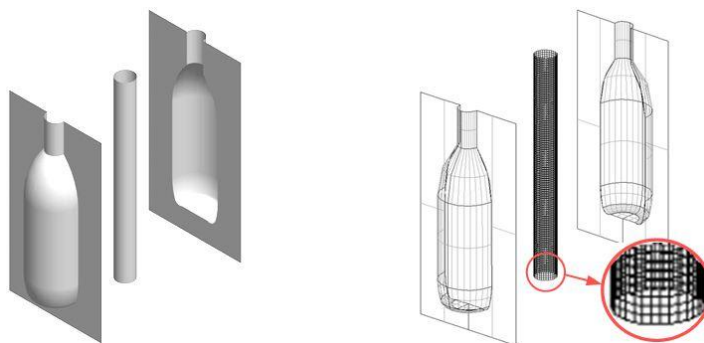


**Fig. 2.** Surface model of the parison and the mold (left), and the corresponding FEM (right).

The parison was created as a cylindrical tube of constant thickness. Its diameter was 28.8 mm, as seen in the left view of Fig. 2. The parison and mold models were transferred to a FEM preprocessing software, MSC. PATRAN 2005, for creating elements and constraints (right view of Fig. 2). The processing used MSC. MARC 2005 for non-linear FEA analysis.

Several preliminary studies were performed to determine the best FEM parameters for the simulation in [14]. For this research, we selected the FEM using full geometry with visco-elastic material model. Since the mold was thick

aluminum alloy, it was assumed to be rigid. The mold temperature deviation during the process was small. These two conditions, rigidity and temperature, allowed no requirement for creating elements at the mold.

The elements of the parison were created using quadrilateral elements with thick shell property. The parison thickness (same as the element thickness) was 2.4 mm. The element size was assigned to be 3 x 3 mm.

The proper size of the element was defined by the area ratio of element (ARE) as

$$ARE = \frac{\text{Element surface area}}{\text{Model surface area}}. \quad (20)$$

Then, the ARE of the FEM was  $3.12 \times 10^{-4}$ ; which was found suitable for the analysis. The summarized detail of the FEM for the parison is shown in Table 1.

**Table 1:** The FEM detail of the parison

Parison	FE Model
Diameter	28.8 mm
Type of element	thick shell
Element thickness	2.4 mm
Shape of element	quadrilateral
Size of element	3 x 3 mm
Area ratio of element, ARE	$3.12 \times 10^{-4}$
Number of node	3232
Number of element	3200

### 3.2 Visco-elastic material condition

The material assigned to elements was both elastic isotropic and thermal isotropic. The material property of HDPE, by using visco-elastic material, was obtained from [15]; they are shown in Table 2 and 3. Table 2 shows the values of  $G_i$  at five shear relaxation times, under a reference temperature of 150°C. The temperature coefficient for shear  $C_{S1}$  and  $C_{S2}$ , of the WLF equation for HDPE between 140°C to 200°C, are shown in Table 3.

**Table 2:** The shear relaxation modulus function  $G_i$  at 150°C of five shear relaxation times,  $\Gamma_i$

$i$	$G_i$ (MPa)	$\Gamma_i$ (sec)	$1 / \Gamma_i$ (sec <sup>-1</sup> )
1	0.245700	0.03906	25.60164
2	0.072430	0.3125	3.2
3	0.030460	2.5	0.4
4	0.007814	20	0.05
5	0.003188	160	0.00625

**Table 3:** The coefficients of the WLF equation for HDPE between 140°C to 200°C

Coefficients	Value
$C_{S1}$	6.928
$C_{S2}$	350
$T_{ref}$	150

The shear relaxation modulus function  $G(t, T)$ , according to Table 2 become

$$G(t, T) = 0.2457e^{-25.60164/b_i} + 0.07243e^{-3.2t/b_i} + 0.03046e^{-0.4t/b_i} + 0.007814e^{-0.05t/b_i} + 0.003188e^{-0.00625t/b_i}. \quad (21)$$

The time-temperature shift function for shear,  $b_t$  or  $b_t(T)$  referring to Eq. (19) and coefficients from Table 3, yield

$$\log [b_t(T)] = -\frac{6.928(T-150)}{350 + (T-150)}. \quad (22)$$

Note that, the temperature  $T$  of Eq. (22) is valid between 140°C to 200°C.

### 3.3 Boundary condition

Fixed constraint was assigned to nodes which has no translation and rotation displacements. For the blowing process, it was applied to nodes at the upper portion of the parison, or the mouth area of the bottle. All other nodes were allowed to move in 6-degree of freedom.

### 3.4 Load and temperature conditions

After the mold was completely closed, the pressure load was assigned inside the parison. The positive pressure supplied the air blowing action. The pressure caused the parison to expand against the mold surface.

The temperature load of 180°C was assigned to the parison temperature. Note that, the melting point of most HDPE is between 115°C and 135°C.

The ambient temperature around the process was given at 30°C, and the mold temperature was set to 25°C. These conditions are shown by the diagram of Fig. 3.

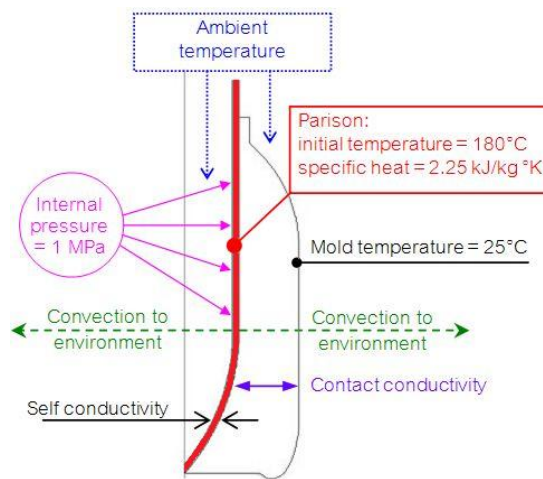


**Fig. 3.** The FEM conditions for simulating the blow molding process.

### 3.5 Contact condition

The two mold-halves need to move at an assigned mold closing speed. The contact condition was applied whenever the elements had contacted the surface of the rigid mold. Note that, the element of the parison was assigned as a deformable body

The first parison area, for the contact condition, was at the lower surface on the parting plane of the mold. It was the portion below the bottom of the bottle, or where the parison was pinch-off. This first contact was during the mold closing process.

The second contact happened during the blowing process. Since the parison elements were thick elements; then the surface representation of the element was in the middle of the thickness or mid-surface. The contact occurred when the elements were moved to the offset distance from the mold surface; this offset was half of the element thickness.

Immediately after the contact, the parison cooled down and solidified, and no more thickness changed. Therefore after the contact, we had to assign no movement of the elements; or they were “glued after contact”. The friction coefficient between the parison and the mold was assigned to infinity.

## 4. RESULTS AND DISCUSSIONS

### 4.1 Blow molding process simulation

The simulation process for extrusion blow molding was separated into two sequences: mold closing process, and followed by blowing process. The FEA simulated the mold closing process is shown in Fig. 4; at time from 0 to 1.0

second. The blue elements indicated no contact with the mold; and yellow color was shown when it contacted the mold. In the actual manufacturing process, after the mold is completely closed, these yellow elements are the pinch-off (as seen in Fig. 4 at time of 1.0 sec).

The blowing process simulation conditions were: 1 MPa for internal pressure, 180°C for the parison temperature and 2.4 mm for the initial parison thickness. The blowing start time was 1.0 second (continued from the final mold closing time of 1.0 second, in Fig. 4). The deforming shapes of the parison, together with the color contour of the thickness at time of 1.0 to 1.6 second are shown in Fig. 5.

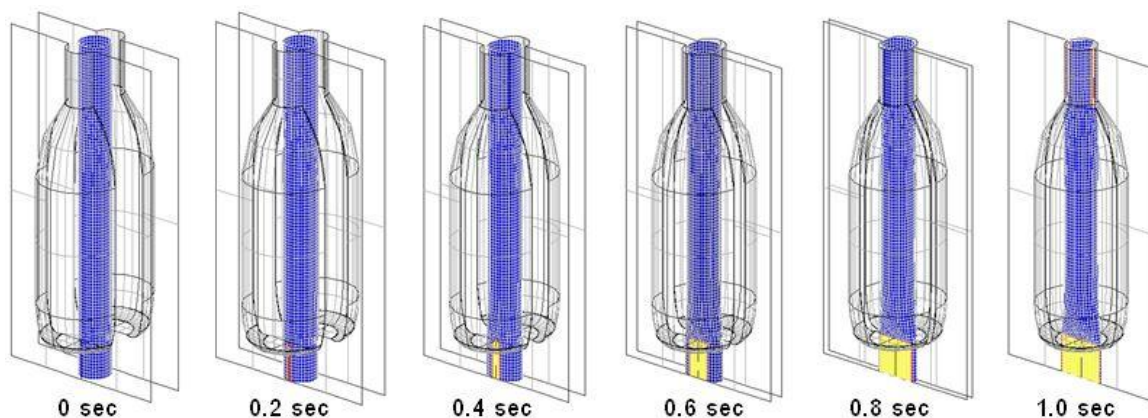


**Fig. 4.** Mold closing times from 0 to 1.0 second. Blue area indicates no contact and yellow vice versa.

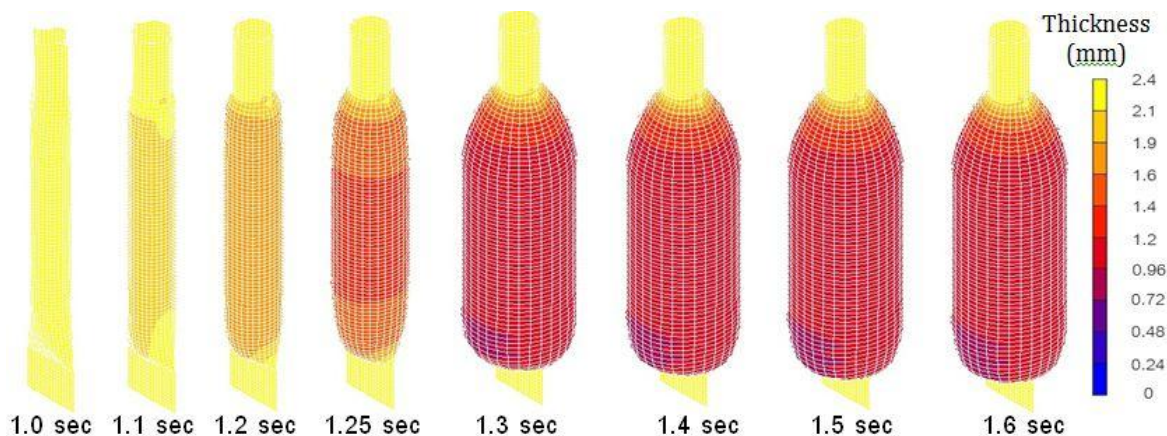


**Fig. 5.** Color contour of the parison thickness, during the blowing process, at times from 1.0 to 1.6 second. The blowing started time is 1.0 second.

#### 4.2 FEA result and the measured wall thickness

The wall thicknesses along the height, of actual bottles, were measured from 5 samples. The locations were on a straight line, on the wall, in the axial direction at 0° from the parting line (Fig. 6). The point at the center of the bottom of the bottle (point “A”) was at zero distance. Point “B” was near the periphery of the base, and point “F” was at the neck of the bottle. The graph of the average and its standard deviation of the measured thickness, at 52 locations on the wall, and the corresponding FEA are shown in Fig. 7. The FEA of Fig. 7 is the parison thickness when it deformed to the shape of the bottle. The FEA result indicated the wall was thicker than the measurement. The errors were caused by: a) the inaccurate of the material constants, b) the exact initial parison thickness, which was difficult to measure, and c) the deviation of the actual processing conditions (for example: the precise value of temperatures and pressure during the process).



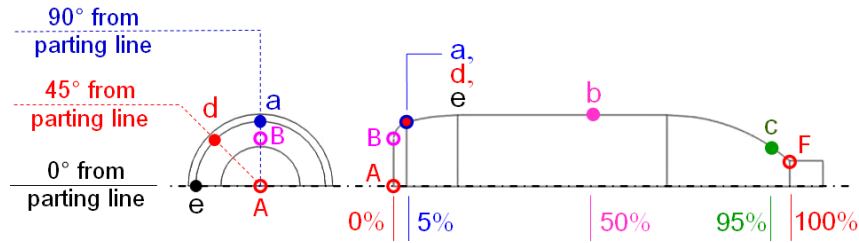


**Fig. 6.** Locations on the wall along the height direction for the thickness analysis.

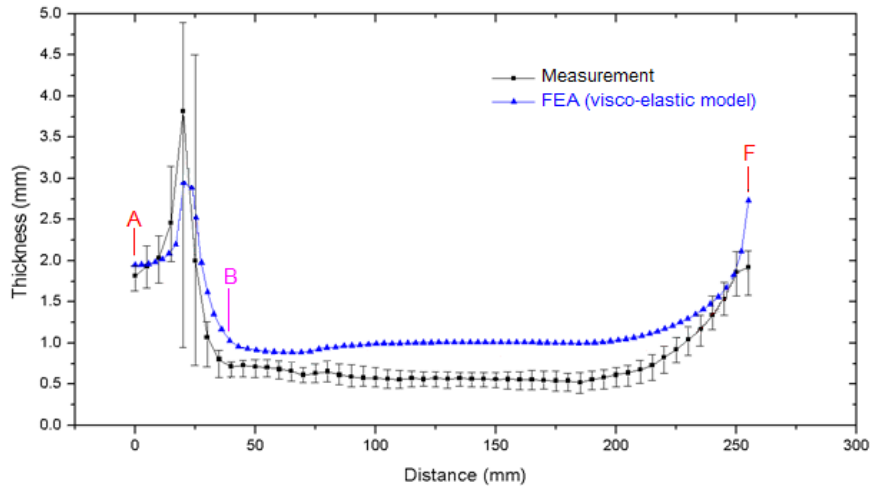


**Fig. 7.** The bottle wall thickness, at 0° from the parting line in the height direction, of the FEA result compared with the averaged thickness of the measurement from five samples.

#### 4.3 Parison thickness analysis result

The locations of interested were at 0°, 45° and 90° from the parting line, as indicated in Fig. 6. The thickness of the parison (before apply the internal pressure) was at 2.2, 2.3, 2.4, 2.5 and 2.6 mm. ( $\pm 2$  mm. from 2.4 mm.). The parison temperature was 180°C and blowing pressure of 1 MPa. The graphs of the thickness profiles corresponding to the percentage of the bottle height at the three angles are shown in Fig. 8a.

The thickness profiles of the five parison thicknesses were similar with each other. For this bottle shape, the thinnest area was near the bottom edge of the bottle; and, the thickest was at the mouth of the bottle.

#### 4.4 Thickness ratio of the parison and the bottle

The thickness ratio (TR) was used for comparing the thickness results from Fig. 8a. The TR was defined as the parison thickness before the process against its final deformed thickness, or the wall thickness of the bottle, that is

$$TR = \frac{\text{Parison thickness}}{\text{Wall thickness of bottle}}. \quad (23)$$

The thickness profiles of Fig. 8a were converted to TR as shown in Fig. 8b. The percent deviation of TR from the parison thickness of 2.4 mm was analyzed from the graphs of Fig. 8b. The average percent of the absolute deviation, along the height, for the thickness of 2.2, 2.3, 2.5 and 2.6 mm is 0.00984%.

Since the percentage deviation is very small (0.00984%), as it could see in Fig. 8b, by the overlapped of all graphs. Under the initial parison thicknesses, from the studies from  $2.4 \pm 0.2$  mm, the TR along the height is considered to be constant at each location along the height.

From this result, the wall thickness of the bottle can be approximated by the use of TR. In this case, we used FEA to calculate the TR from one selected parison thickness; the other final bottle wall thickness could be obtained by dividing the required parison thickness by TR.



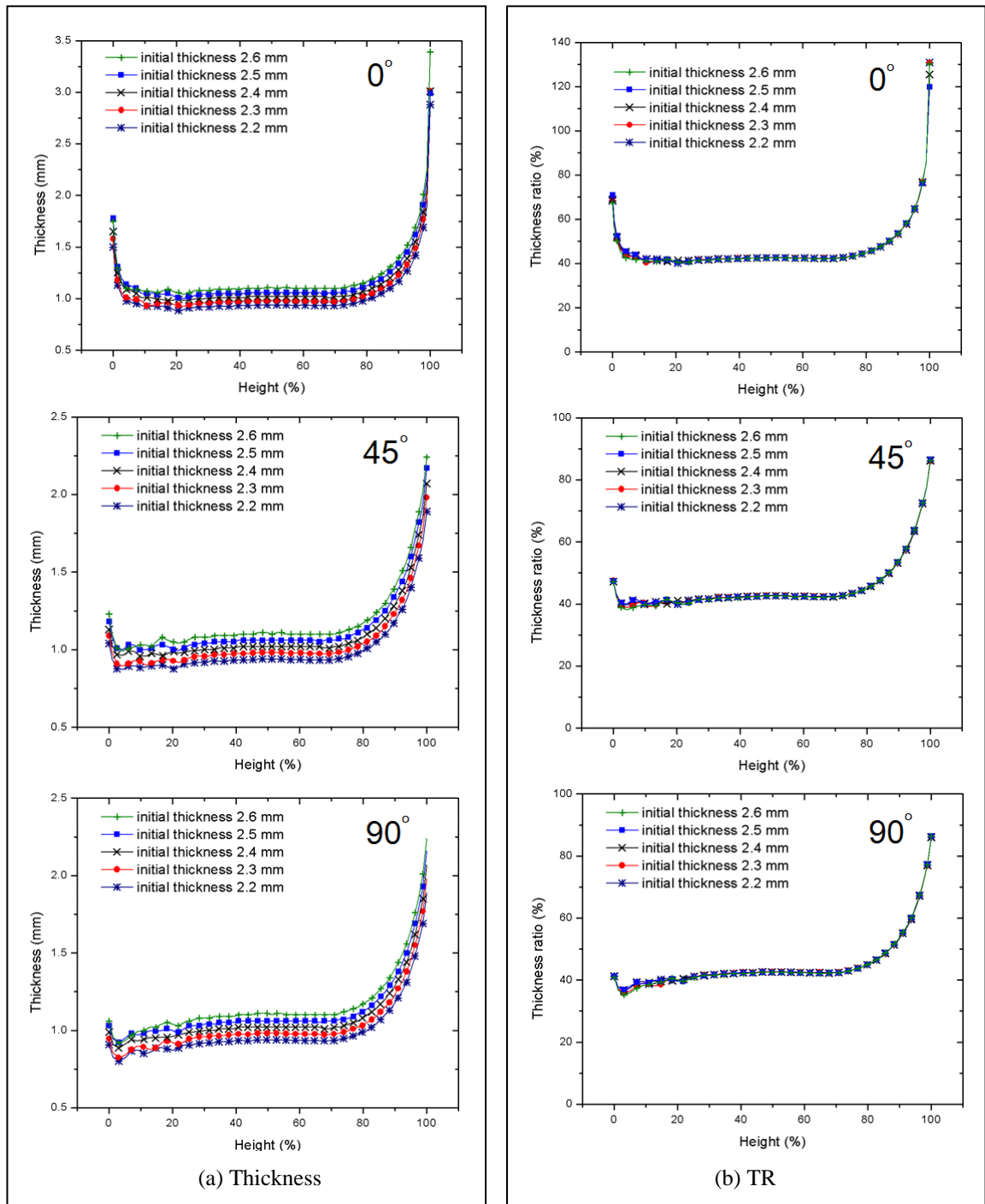


**Fig. 8.** a) Comparing the wall thickness, and b) the percent thickness ratio, TR, against the percent bottle height. The parison thicknesses are 2.2 to 2.6 mm at 0°, 45° and 90° from the parting line.

#### 4.5 Parison thickness variation in time

The following conditions were used for analyzing the thickness during the extrusion blow molding process; they were: parison temperature of 180°C, pressure of 1 MPa, parison thickness of 2.4 mm, and the blowing period of 1.0 second. The color contour of the thickness was the same as Fig. 5.

The thickness was observed at three points (“a”, “b” and “c” in Fig. 6) on the wall of the bottle, at 5%, 50% and 95% of the bottle height; all at the angle of 90° from the parting line, as shown in Fig. 9.

Due to the heat transfer from the parison to the mold, the parison temperature started decreasing. The parison was solidified to the shape of the mold when the temperature was below the hardening temperature. The final parison thickness could be seen from the graph, of Fig. 9, when it became constant. The graph also indicated that the location where the parison made the first contact (point “c”) had thicker thickness than those later (point “b” and “c”, respectively). Notice that the time 1.38 second was the parison-contact-time of point “a”.

The thickness of the three points at 5% of the height, and 0°, 45° and 90° from the parting line (point “a”, “d” and “e” in Fig. 6), are shown in Fig. 10. The graphs in Fig. 10 indicated the thickness at point “e” was the thickest (comparing to point “a” and “d”); because this point was on the parting line or the pinch-off location.

The table summarized the parison-contact-time and the corresponding thicknesses of point “a” to “e” are shown in Table 4.

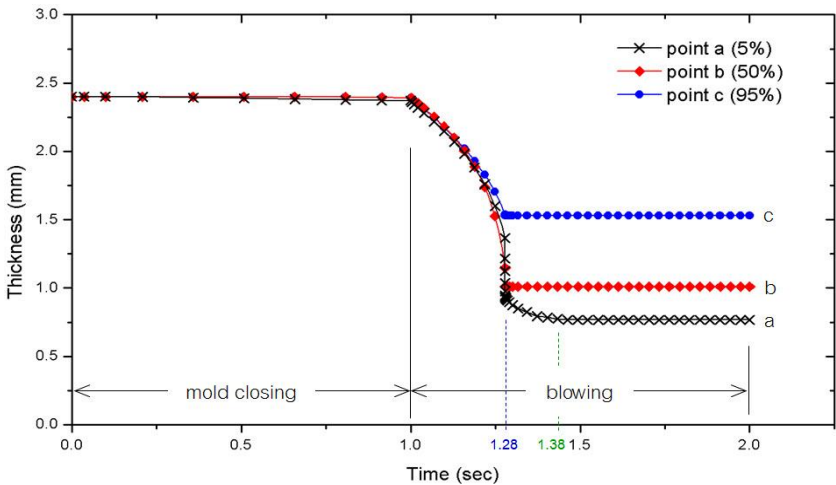


**Fig. 9.** The thickness variation in time at points: 5%, 50% and 95% of the height, and 90° from the parting line.

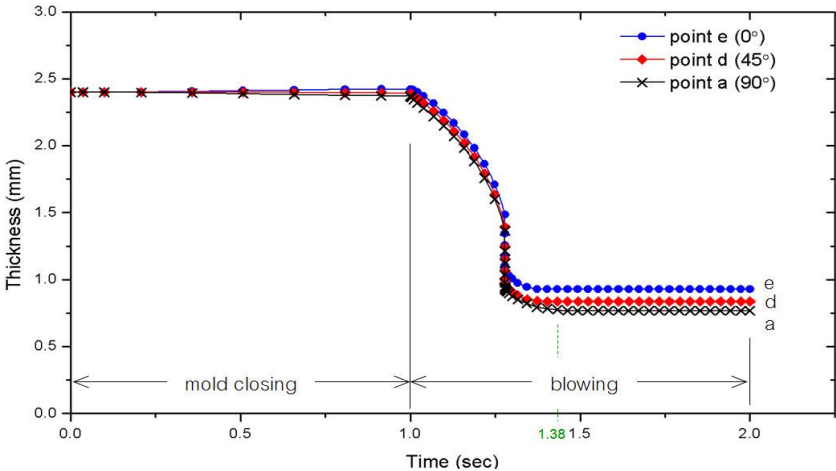


**Fig. 10.** The thickness variation in time at point 5% of the height, and the angle of 0°, 45° and 90° from the parting line.

**Table 4:** Comparing the parison-contact-time and thickness at the five points on the bottle

Point	Location		Parison	
	Height (%)	Angle (deg.)	Contact time (sec)	Thickness (mm)
a	5	90	1.3831	0.76701
b	50	90	1.2785	1.01116
c	95	90	1.2785	1.53028
d	5	45	1.3531	0.83536
e	5	0	1.3431	0.92860

Point “a”, represented the location at 5% of the height and 90° from the parting line, indicated longer time for the thickness to become steady or constant. This point “a” was near the bottom edge of the bottle, as expected, it was found to be the thinnest.

#### 4.6 Parison temperature variation in time

The resulting temperature graphs at point “a”, when the initial parison temperature were at 160°C, 180°C and 200°C are shown in Fig. 11. Note that, the point “a” was the location where the parison took the longest time to become steady.

The graphs in Fig. 11 showed the temperature versus time of the three initial parison temperatures. As expected, when the parison temperature is increased, the time to cool down to the ambient temperature is also increased. If the hardening temperature is known, the graph can be used to determine the time for mold opening.

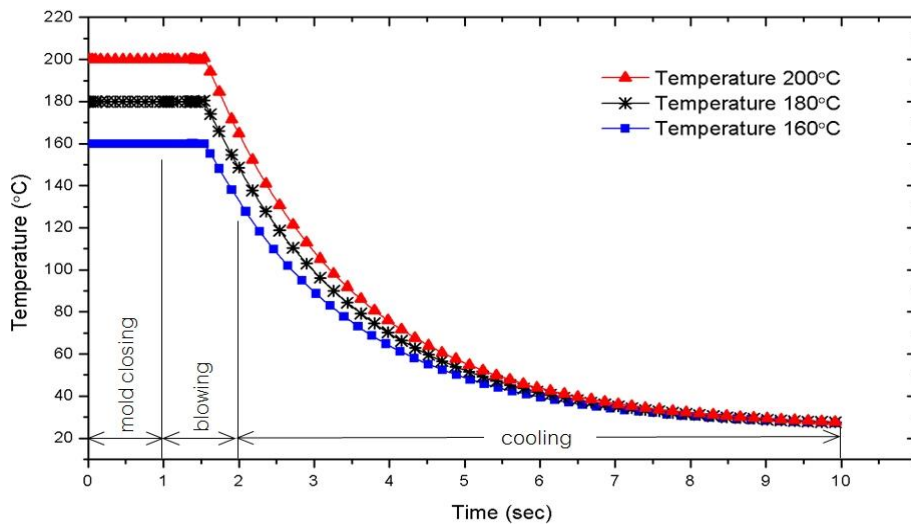


**Fig. 11.** Comparing the thickness at point “a” when the parison temperatures were at 160°C, 180°C and 200°C.

Graphs of the thickness and temperature varied with time at point “a” were plotted together as shown in Fig. 12. The graph of the temperature in Fig. 12 allows us to determine the time taken the parison to become solid, and the time taken the thickness to be uniform. It is evident that the parison temperature started to decrease when the parison began to make a contact with the mold. This means that the hardening time always longer than the time taken the parison to be uniformed.

For a HDPE with the hardening temperature of 130°C, the hardening time is graphically obtained from the graph, of Fig. 12; the time is around 2.3 second. While the parison-contact-time is 1.32 second. Without consideration the mold opening time, the cycle time for the blowing process will be 2.3 second.

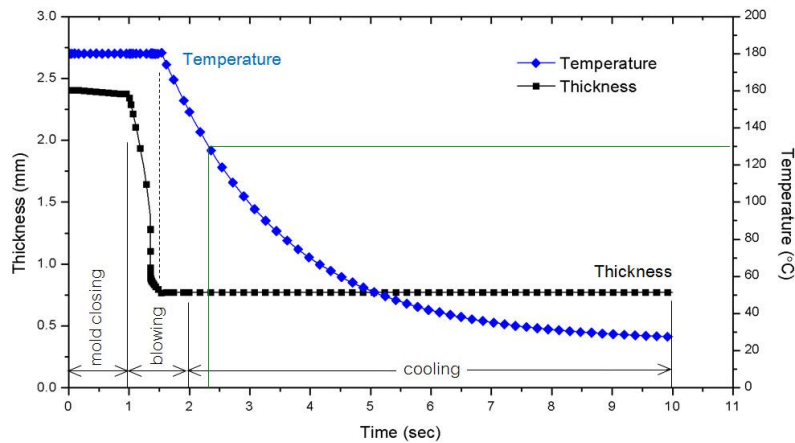


**Fig. 12.** Graph shown the thickness and temperature, at point “a”, when the initial temperature is 180°C, and the initial thickness of 2.4 mm.

## 5. CONCLUSION

The time variation of thickness and temperature, during the extrusion blow molding process, were examined by using visco-elastic mathematical model for the HDPE. The FEM of the bottle was found to have the area ratio of element (ARE) of  $3.12 \times 10^{-4}$ ; which gave the suitable element size for the analysis. The thickness ratio (TR) of the axis-symmetric bottle shape was constant, or uniform along the height, in the simulated parison thickness between 2.2 to 2.6 mm. The information from the TR is useful for predicting the bottle thickness when the parison thickness is changed; therefore, the wall thickness of bottle is  $TR^{-1}$  multiply by parison thickness. The graph of the thickness variation over time at points on the bottle was analyzed; it started from mold closing to blowing, and until no changed in the thickness. The time variation plot of the temperature and thickness, at the point with the thinnest thickness, is useful for predicting the cycle times of the process.

## 6. ACKNOWLEDGEMENTS

This work was done and used the CAD and FEA softwares in the Mechanical and Product Design Research Laboratory (MPDRL) at the Department of Mechanical Engineering, Faculty of Engineering, Kasetsart University. This work was supported by grants MRG-WI525E030 from the Thai Research Fund (TRF), and Panjawatana Plastic Co., Ltd.

## NOMENCLATURE

ARE	area ratio of element, dimensionless
$a_t(T)$	time-temperature shift function
$b_t(T)$	shear time-temperature shift function
CAD	Computer-Aided Design
$C_1$	temperature coefficient, dimensionless
$C_2$	temperature constant, °C
$C_{S1}$	shear temperature coefficient, dimensionless
$C_{S2}$	shear temperature constant, °C
E	elastic modulus, Pa
$E(t)$	stress relaxation modulus function of time, Pa
$E(t, T)$	stress relaxation modulus function of time and temperature, Pa
FEA	Finite-Element Analysis
FEM	Finite-Element Model
$G(t)$	shear relaxation modulus function of time, Pa
$G(t, T)$	shear relaxation modulus function of time and temperature, Pa
HDPE	high density polyethylene
TR	thickness ratio, dimensionless

$t$	time, second
$T$	temperature, °C
WLF	Williams-Landel-Ferry
$\varepsilon$	strain, dimensionless
$\dot{\varepsilon}$	strain rate, sec <sup>-1</sup>
$\eta$	viscosity, Pa·sec
$\sigma$	stress, Pa
$\tau$	relaxation time, second
$\Gamma$	shear relaxation time, second

#### Subscripts

$e$	elastic
ref	reference
s	shear
$t$	time
$v$	viscous

#### REFERENCES

- [1] Lee, N.C. Blow Molding Design Guide, Carl Hanser Verlag, 1998.
- [2] Lee, N.C. Plastic Blow Molding Handbook, Van Nostrand Reinhold, 1990.
- [3] Liu, S.J. Computer simulation of the inflation process in blow molding, Journal of Reinforced Plastics and Composites, Vol. 18(8), 1999, pp. 759-774.
- [4] Fukuzawa, Y., Tanoue, S., Iemoto, Y., Kawachi, R. and Tomiyama, H. Three-dimensional simulation on multilayer parison shape at pinch-off stage in extrusion blow molding, Polymer Engineering & Science, Vol. 50(7), 2010, pp. 1476-1484.
- [5] Gupta, S., Uday, V., Raghuwanshi, A.S., Chowkshey, S., Das, S.N. and Suresh, S. Simulation of blow molding using ANSYS Polyflow, APCBEE Procedia, Vol. 5, 2013, pp. 468-473.
- [6] Huang, H., Li, J., Li, D. and Huang, G. New strategies for predicting parison dimensions in extrusion blow molding, Poly-Plastics Technology and Engineering, Vol. 50(13), 2011, pp. 1329-1337.
- [7] Cosson, B., Chevalier, L. and Regnier, G. Simulation of the stretch blow moulding process: from the modelling of the microstructure evolution to the end-use elastic properties of polyethylene terephthalate bottles, International Journal of Material Forming, Vol. 5, 2012, pp. 39-53.
- [8] Zimmer, J. and Stommel, M. Method for the evaluation of stretch blow molding simulations with free blow trials, IOP Conference Series: Materials Science and Engineering, Vol. 48, 2013, Article ID 012004.
- [9] Bougharriou, A., Jeridi, M., Hdiji, M., Boughrira, A. and Sai, S. Finite element analysis of PMMA stretch blow molding, International Journal of Manufacturing Engineering, 2014, Article ID 175743.
- [10] Mase, G.T., Smelser, R.E. and Mase, G.E. Continuum Mechanics for Engineers, 3<sup>rd</sup> edition, CRC Press, 2010.
- [11] Rugsaj, R., Thusneyapan, S. and Suvanjumrat, C. Finite element models for analysis the parison thickness of extrusion blow molding process, 6<sup>th</sup> TSME International Conference on Mechanical Engineering, Petchburi, Thailand, 2015, Article ID CST5.
- [12] Shames, I.H. and Cozzareli, F.A. Elastic and Inelastic Stress Analysis, Prentice-Hall, 1992.
- [13] Ferry, J.D. Viscoelastic Properties of Polymers, 3<sup>rd</sup> edition, John Wiley & Sons, 1980.
- [14] Rugsaj, R. Parison Thickness Analysis for Extrusion Blow Molding, ME thesis, Kasetsart University, Bangkok, Thailand, 2014.
- [15] Larocche, D., Kabanemi, K.K., Pecora L. and Diraddo, R.W. Integrated numerical modeling of the blow molding process, Polymer Engineering & Science, Vol. 39(7), 1999, pp. 1223-1233.